Impact of Parallel Micro-Engineered Stent Grooves on Endothelial Cell Migration, Proliferation, and Function

An In Vivo Correlation Study of the Healing Response in the Coronary Swine Model

Eugene A. Sprague, PhD; Fermin Tio, MD; S. Hinan Ahmed, MD; Juan F. Granada, MD; Steven R. Bailey, MD

Background—Stent luminal surface characteristics influence surface endothelialization. We hypothesize that luminal stent microgrooves created in the direction of coronary flow accelerate endothelial cell migration, resulting in lower levels of neointimal formation.

Methods and Results—Surface coverage efficiency was evaluated in vitro by allowing human aortic endothelial cells (HAEC) to migrate onto microgrooved (G) or smooth (NG) surfaces. HAEC functionality was assessed by proliferation rate, apoptosis rate, nitric oxide production, and inflammatory markers TNF-α and VCAM-1 expression. Early endothelialization and restenosis studies were performed using the porcine coronary injury model. Stainless steel stents of identical design with (GS) and without (NGS) luminal microgrooves were used. The commercially available Multi-Link Vision (MLVS) stent of identical design was used as a control. The degree of GS and NGS surface endothelialization was compared at 3 days. Biocompatibility and tissue response outcomes were evaluated at 28 days. The in vitro study demonstrated that at 7 days the presence of surface microgrooves increased HAEC migration distance >2-fold. Cell proliferation rate and nitric oxide production were increased and apoptosis rate was decreased. There was no difference in inflammatory marker expression. At 3 days, coronary artery stent endothelialization was significantly increased in GS compared with NGS (81.3% versus 67.5%, P=0.0002). At 28 days, GS exhibited lower neointimal thickness compared with either NGS (21.1%, P=0.011) or MLVS (40.8%, P=0.014).

Conclusions—Parallel microgrooves on coronary stent luminal surfaces promote endothelial cell migration and positively influence endothelial cell function, resulting in decreased neointimal formation in the porcine coronary injury model. ***(Circ Cardiovasc Interv.* 2012;5:499-507.)**

Key Words: coronary stent ■ endothelial function ■ endothelialization ■ neointimal hyperplasia ■ restenosis

Drug-eluting stents (DES) have dramatically reduced the long-term rate of reintervention and improved clinical outcomes among patients undergoing percutaneous coronary interventions.[1] However, DES use still carries a small but critically important cumulative risk of late stent thrombosis. Human pathology studies suggest that delayed healing leads to incomplete strut coverage, which has been associated with late thrombotic events.[2] Moreover, early DES platforms elicited enhanced platelet adhesion[3] and endothelial dysfunction.[4]

Most DES technologies now embody thinner metallic platforms containing minimal amounts of polymeric drug formulations while maintaining drug concentrations and release profiles.[5,6] Although a slight decline in the overall stent thrombosis rate has been observed with the use of latest generation of DES platforms, these potentially lethal events still occur. Despite their efficacy in preventing restenosis, the antiproliferative effect of drugs used in commercially available DES appear to delay stent endothelialization. Technological approaches have been used to enhance stent endothelialization by modifying the stent surface with antibodies to selectively bind circulating endothelial progenitor cells.[7] An alternate strategy to encourage reendothelialization is to modify the stent surface to increase the natural rate of endothelial cell migration from adjacent arterial areas of intact healthy endothelium. Previous studies in our laboratory have shown that parallel microgrooves applied to the surface of different metals[8,9] increase the rate of human aortic endothelial cell migration by >2-fold compared with smooth coupons. More importantly, when this pattern was applied to the luminal surface of stents in an early pilot study, the endothelialization rate on these grooved stents was double compared with

Received December 22, 2011; accepted May 31, 2012.

From the University of Texas Health Science Center at San Antonio, San Antonio, TX (E.A.S., F.T., S.H.A., S.R.B.); and Skirball Center for Cardiovascular Research, Cardiovascular Research Foundation, Columbia University Medical Center, New York, NY (J.F.G.).

Correspondence to Eugene A. Sprague, PhD, Department of Medicine/Division of Cardiology, University of Texas Health Science Center at San Antonio, 7703 Floyd Curl Dr, San Antonio, TX 78229. E-mail sprague@uthscsa.edu

Circ Cardiovasc Interv **is available at http://circinterventions.ahajournals.org** **DOI: 10.1161/CIRCINTERVENTIONS.111.967901**

smooth surface stents when implanted in pig carotid arteries.[9] In the present study, we aim to demonstrate that parallel microgrooves applied to the luminal stent surface effectively enhances endothelial cell (EC) migration both in vitro and in vivo. Furthermore, we seek to demonstrate that the increased rate of reestablishment of an intact endothelium is associated with a decrease in neointimal formation compared with arteries receiving a similar stent design with no surface patterning in the porcine coronary injury model.

WHAT IS KNOWN

- Restoration of an intact functional endothelium at stented revascularization sites limits thrombosis and arterial wall remodeling.
- Stent surface biocompatibility influences the endothelialization rate and restoration of implanted stents.
- Current drug-eluting stents inhibit restoration of a functional endothelium.

WHAT THE STUDY ADDS

- A patterned microgrooved stent surface can increase the rate of surface endothelialization.
- Increasing the rate of reendothelialization using a microgrooved stent is associated with decreased intimal hyperplasia.

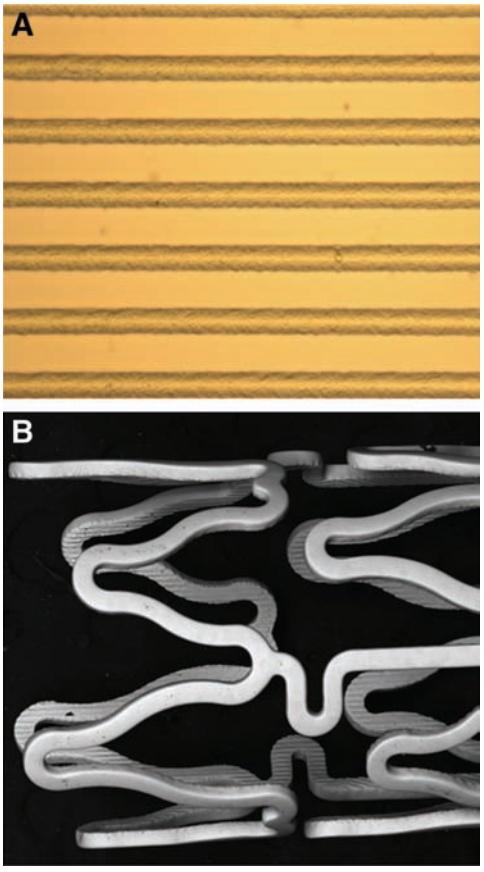

Figure 1. A, Photomicrograph of a grooved coupon with alternating 15-μm-wide grooves used for human aortic endothelial cell migration studies. **B**, Scanning electron micrograph of a stent with a luminal surface composed of alternating 15-μm-wide grooves.

Methods

In Vitro Studies

Test Surface Preparation

Based on previous studies indicating optimum endothelial cell migration on surfaces patterned with 15-μm wide grooves, cobalt chromium (L605) and 316 L stainless steel grooved coupons (1x1 cm) were created using a proprietary chemical etching-based process. The physical characteristics of the grooves were analyzed by light and scanning electron microscopy yielding a groove width of 14±3 μm with an intervening space of 15±3.5 μm. The depth of the grooves was measured to be 2±0.5 μm. Patterning was consistent across all specimens. A typical patterned specimen is shown in Figure 1A. Flat, electropolished, smooth surface coupons of the same material and dimensions were prepared as controls.

EC Migration Studies

Human aortic ECs (HAEC) obtained from Cascade Biologicals, Inc, were cultured in MCDB 131 culture medium (Sigma-Aldrich, Inc, St Louis, MO) containing 10% iron-supplemented calf serum (Hyclone Laboratories, Inc, Logan, UT). Endothelial cell migration experiments were conducted using the in vitro arterial wall migration model established in our laboratory.[10] In brief, a model arterial surface is created using a 1% vol/vol collagen type I solution (Collaborative Research, Waltham, MA) cross-linked with ammonium to form a 2-mm-thick firm gel. HAEC are seeded and cultured to attain confluence within 1 day. Sterile test materials are implanted onto the cell covered gel such that the top surface is flush with the surrounding gel surface and incubated at 37°C for 7 days to allow cell migration on to the test surfaces. Cell migration distance was measured as the perpendicular distance from the midpoint of each coupon edge to the leading edge of migrating cells toward using a microscope-based micrometer. HAEC focal adhesion sites on migrating cells were identified by anti–p-focal adhesion kinase (pFAK), which specifically labels active adhesion sites involved in cell migration, and were quantified by reflective light microscopy. The functionality of the migrating cells was assessed by cell proliferation rate, apoptosis rate, and nitric oxide (NO) production. HAEC proliferation was identified using fluorescently tagged anti–proliferating cell antigen (anti-PCNA) and quantified microscopically as percentage of labeled nuclei. Apoptosis was quantified using the Annexin V-FITC–based Vibrant apoptosis detection kit (Life Technologies, Grand Island, NY). Intracellular NO level was determined using the fluorescent NO indicator DAF-FM.[11] To verify NO identification, migrating HAEC on both surfaces were preincubated with the specific NO synthase inhibitor L-NAME (0.5 mmol/L) as a negative control.[12] Expression of inflammatory markers TNF-α and VCAM-1 was detected using fluorescently tagged specific antibodies (Life Technologies).

In Vivo Studies

Study Design

To explore the hypothesis that grooved stents (GS) promote accelerated surface endothelialization along with limiting neointimal formation, the animal study was divided into 3 comparison groups of 8 animals each. The overall study design is presented in the flow chart in Figure 2. In the first group, a total of 8 animals received paired GS and non-GS (NGS) in a 3-day study to evaluate the overall stent endothelialization rate. In the second group, 8 pigs received paired GS and NGS and 8 pigs received paired and Multi-Link Vision stents (MLVS; Abbott Vascular). These 16 animals were evaluated at 28 days for degree and quality of neointimal formation. Paired stents were randomly implanted in a side-to-side fashion in the right or left anterior descending coronary arteries of domestic swine using a conventional overstretch injury model.[13] All implanted

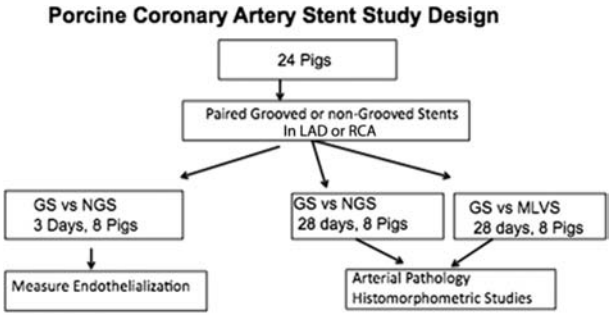

Figure 2. Design for porcine coronary artery paired comparison studies of the grooved stent (GS) with either the nongrooved stent (NGS) of the same design or the commercial Multi-Link Vision stent (MLVS). LAD indicates left anterior descending artery; RCA, right coronary artery.

stents (GS, NGS, and MLVS) were 15 mm in length. The target site was selected by using quantitative coronary angiography. All stents were mounted on an identical balloon dilatation catheter (Voyager 2.75, Abbott Laboratories) and were dilated to achieve 10% overstretch ratio, based on angiographic measurements.

Stent Description

Both GS and NGS stents were manufactured using current industrial processing, leading to identical stent designs (Palmaz Scientific) based on a design identical to the commercial MLVS (Abbott Laboratories Chicago, IL). These stents were laser-cut from 316L stainless steel tubing rather than cobalt chromium alloy base used in the MLVS. MLVS stents were used as supplied by the manufacturer for clinical use. GS surfaces were processed to have the same groove pattern and dimensions as described above for the grooved coupon surfaces (Figure 1B).

Procedural Description

The study protocol was approved by the University of Texas Health Science Center at San Antonio IACUC. All animals were fed a standard diet and premedicated with Norvasc (5 mg/d), clopidogrel (75 mg), and aspirin (325 mg) orally 24 hours before each procedure. Juvenile domestic Yorkshire pigs (weight, 30–40/kg) were induced with Telazol (3–5 mg/kg IM) and anesthetized with isoflurane (1% to 3% in 100% O_2). Before cardiac catheterization, heparin (5000 to 10 000 U) was injected to maintain an activated clotting time of 250 to 300 seconds. Nitroglycerin was administered intra-arterially to prevent or relieve vasospasm. The appropriate stent was delivered to the intended site over a guide wire under fluoroscopic guidance, and stent deployment was performed as described above. Animals were recovered from anesthesia and maintained on aspirin, Norvasc, and clopidogrel for 2 weeks, with aspirin continued until their designated day of euthanasia.

Histology Analysis

The animals were euthanized under general anesthesia by intravenous injection of pentobarbital euthanasia solution (100 mg/kg), after heparinization. Hearts were excised and pressure-perfused with 0.9% saline until cleared of blood, followed by pressure-perfusion fixation in 10% neutral-buffered formalin. The stented vessels were dehydrated in a graded series of ethanol and embedded in methylmethacrylate. In the 3-day study group, the coronary arteries were flushed with 0.1% silver nitrate solution before fixing to facilitate identification of the endothelial cell coverage. In long-term studies (28 days), the hearts were removed after 28 days, fixed, and submitted for histopathology. The 3-day stent specimens were sectioned every 1.5 mm, and each of 9 consecutive serial cross sections from the proximal to the distal end were analyzed for the extent of endothelial coverage. Endothelial coverage was quantified and expressed as percentage of the lumen circumference covered by endothelium. The 28-day specimens yielded 5 cross sections; taken every 3 mm along the stent length. Histological analysis focused on endothelial cell coverage in the 3-day specimens and on assessment of intimal area, thickness, injury, and inflammatory reaction in 28-day specimens. Five- to 6-μm sections were cut on a rotary microtome and stained with hematoxylin and eosin and elastic Van Gieson stain. A vessel injury score was calculated as described by Schwartz.[13] The cross-sectional areas (as subtended by the internal elastic lamina, and the lumen) of each section were mapped and measured by digital morphometry. Neointimal thickness was measured as the distance from the inner surface of each stent strut to the luminal border. An overall neointimal inflammation value (0–4) and fibrin value (0–3) were scored for each section.

Statistical Analysis

Continuous data obtained within in vitro studies were expressed as mean±SD, and statistical comparisons were performed using the Student unpaired *t* test; arterial endothelialization was compared using the paired *t* test. Statistical comparison of the porcine arterial histology parameters were performed using both Students paired *t* test and Wilcoxon signed-rank tests. A probability value of <0.05 was considered statistically significant.

Results

In Vitro Studies

Endothelial migration rate was assessed using the in vitro arterial wall model described above. HAEC migration distance across the grooved stainless steel cobalt chromium surfaces over a 7-day period was >2-fold higher (n=6, $P<0.001$) compared with that observed on the nongrooved control (Figure 3A through 3C). Consistent with these increases in migration, active focal adhesion site density (FAS/cell) was significantly (n=6, $P<0.001$) increased 2-fold in HAEC migrating on grooved compared with smooth stainless steel (Figure 3D through 3F). FAS density in HAEC migrating on grooved compared with smooth cobalt chromium surfaces was also significantly increased (n=6, $P=0.034$).

The functionality of the more rapidly migrating cells on GS surfaces was assessed using key markers of endothelial physiology. HAEC proliferation rate was nearly double (35.7 versus 19.8%, $P<0.001$) and increased by nearly 50% (31.4 versus 22.4, $P=0.044$) for cells migrating on grooved compared with nongrooved stainless steel and cobalt chromium, respectively (Figure 4A through 4C). Cell apoptosis rates were significantly reduced by >80% for HAEC migrated on grooved specimens relative to the respective smooth surfaces (Figure 4D through 4F). Interestingly, apoptosis rates were significantly elevated in cells that migrated onto nongrooved cobalt chromium surface compared with stainless steel. In addition, there was a nearly 25% increase ($P<0.001$) in NO production on cells migrating onto grooved surfaces compared with cells on nongrooved surfaces (Figure 4G through 4J). This increase in NO was blocked by a 30-minute preincubation with the inhibitor L-NAME. There was no evidence of VCAM-1 and TNF-α cell expression (cell activation to a proinflammatory status) in cells on any surface.

In Vivo Stent Endothelialization Study

In the 3-day animal studies, a significant increase in endothelial coverage on GS compared with NGS was observed. As depicted in Figure 5A, an average 81.3% of the total GS surface was covered with endothelial cells compared with 67.5% for the NGS group ($P=0.0002$). A line plot of the average endothelial coverage at each individual cross section

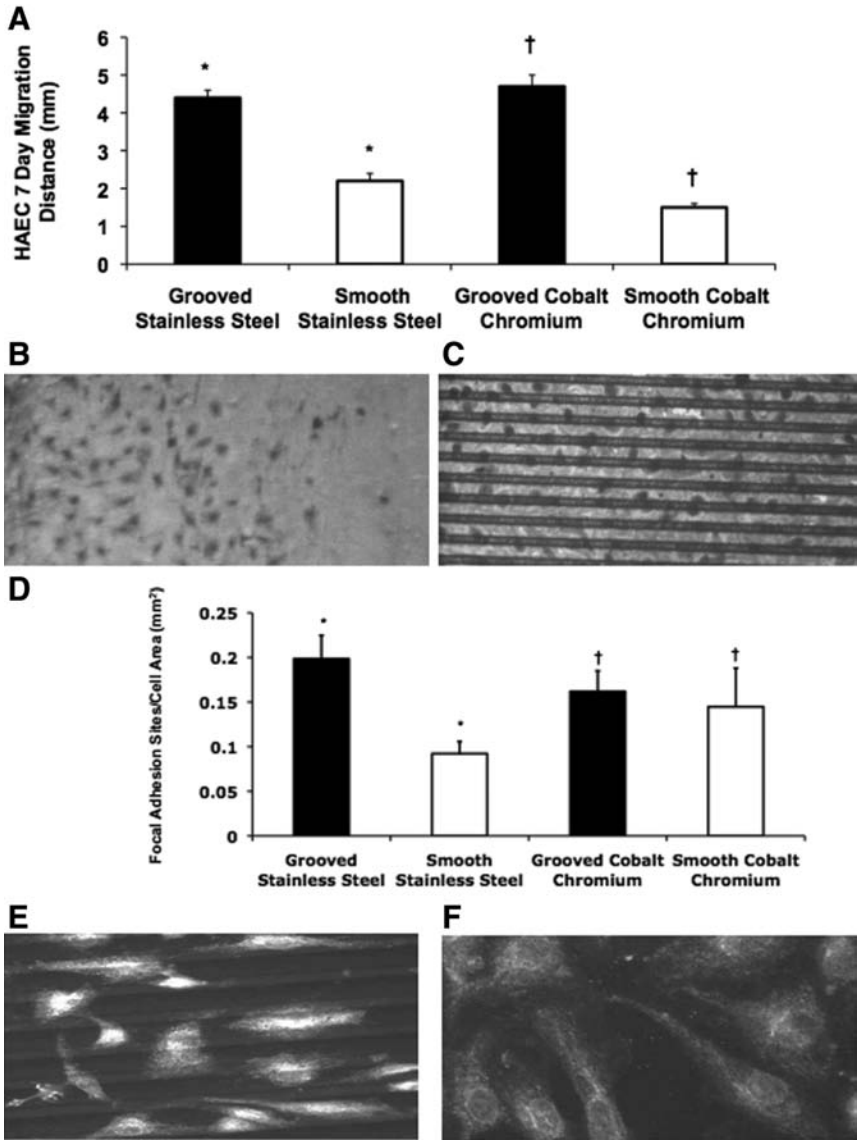

Figure 3. **A**, Human aortic endothelial cell (HAEC) migration distance on to grooved or smooth surface stainless steel or cobalt chromium over 7 days. Values are expressed as mean±SD; n=6; **P*<0.001, †*P*<0.001. **B** and **C**, Representative photomicrographs of **B**, a confluent HAEC migration along a segment of a completely endothelialized grooved surface (**C**) leading edge of HAEC migration at 2 mm from the edge of smooth cobalt chromium surface (magnification ×100). **D**, Focal adhesion sites per migrating HAEC that have migrated onto grooved or smooth surface stainless steel or cobalt chromium coupons (day 7). Focal adhesion sites (FAS) are identified by immunofluorescent labeling of phosphorylated focal adhesion kinase. Values are expressed as mean±SD; n=6; **P*<0.001,†*P*=0.034. **E** and **F**, Representative photomicrographs depicting a greater density of fluorescently labeled FAS within migrating HAEC on grooved (**E**) compared with smooth (**F**) stainless steel coupons (magnification ×200).

(9 sections) along the stent length showed all levels had greater in-stent EC coverage for GS compared with NGS (Figure 5B). Also, there were an increased but not statistically significant number of inflammatory cells observed within NGS compared with GS (2.37 versus 1.67 cells per section, *P*=0.066). No thrombus formation on stent struts was observed. Representative complete and strut cross sections obtained at comparable levels along GS and NGS illustrating the degree of endothelial coverage are presented in Figure6A through 6D.

Twenty-Eight–Day Outcome Analysis

The outcome analyses results are presented in Tables 1 and 2. Average injury scores were low (<1) for all groups. Also, stent final diameter measured at study end was similar among all treated groups. The results indicate that average neointimal area and thickness were significantly lower within the GS compared with both NGS and MLVS groups, as shown in representative images within Figure 7A and 7B. Specifically, neointimal proliferation response as measured by neointimal thickness was 21.1% and 40.8% lower for GS compared with the NGS and the MLVS group, respectively. Consistent with these observations, GS sites retained a larger lumen diameter and a significantly decreased percent stent lumen area occlusion compared with either the NGS or MLVS groups. Although there was no significant difference in inflammation, injury, or fibrin scores observed between GS and NGS areas, MLVS areas displayed higher fibrin and inflammatory scores compared with the GS groups. No thrombus formation was observed on stent struts in any group.

Discussion

Several large, randomized, controlled trials have demonstrated the efficacy of different DES in reducing restenosis among patients undergoing percutaneous coronary interventions. However, despite significant advances that have been made in development of the latest generations of DES platforms, very late stent thrombotic events continue to occur.[14] An intact functional endothelial lining is critical to

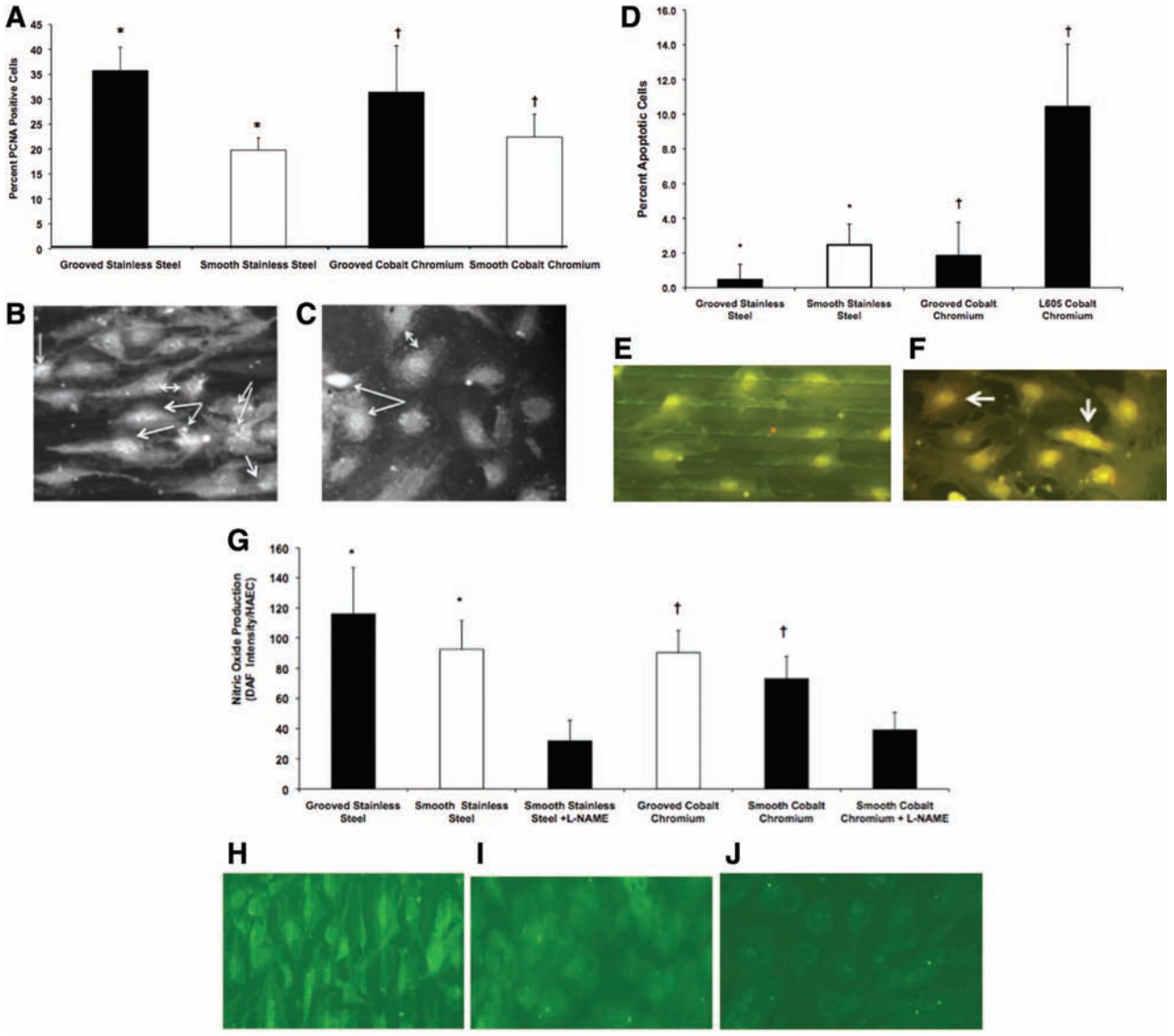

Figure 4. **A**, Endothelial cell proliferation rate for cells that have migrated on to grooved or smooth stainless steel or cobalt chromium coupons as measured by percent anti-PCNA fluorescently labeled nuclei at day 7. Values are expressed as mean±SD; n=6; **P*<0.001, †*P*=0.044. **B** and **C**, Representative photomicrographs depicting a higher percent anti-PCNA fluorescently labeled nuclei (**arrows**) within migrating human aortic endothelial cell (HAEC) on grooved (**B**) compared with smooth (**C**) stainless steel surfaces. **D**, Apoptosis rate for HAEC that have migrated on to grooved or smooth stainless steel or cobalt chromium coupons at day 7 as measured by an annexin V–based apoptosis assay. Values are expressed as mean±SD; n=6; **P*<0.001, †*P*<0.001. **E** and **F**, Representative photomicrographs depicting apoptosis assay of migrating HAEC on grooved (**E**) and smooth (**F**) cobalt chromium surfaces. **Arrows** and faint orange stain identify apoptotic cells. **G**, Endothelial nitric oxide (NO) production for cells that have migrated on to grooved or smooth stainless steel or cobalt chromium coupons as measured by the DAF-FM method at day 7. Values are expressed as mean±SD; n=6; **P*<0.001, †*P*<0.001. **H** through **J**, Representative photomicrographs depicting increased NO production in HAEC on grooved stainless steel (**H**) without inhibitor as detected by DAF-FM compared with HAEC on smooth surfaces pretreated without (**I**) and with (**J**) the specific NO inhibitor L-NAME and (magnification ×200).

provide a nonthrombogenic surface and maintenance of arterial function and architecture. Thus, rapid restoration of an intact endothelium at stented arterial sites is an essential consideration in DES development and implantation.

An alternate strategy to accelerate endothelialization is to provide a defined grooved topography on the stent surface to direct and facilitate migration of adjacent arterial endothelium into the stented area. Previous studies in our laboratory have demonstrated that parallel microgrooves applied to the surface of either nitinol[8] or 316L stainless steel[9] increase the rate of HAEC migration by >2-fold compared with unpatterned surfaces in vitro. More importantly, when this microgrooved pattern was applied to the luminal surface of stents, the endothelialization rate on these grooved stents was double that observed for smooth surface stents when implanted in pig carotid arteries.[9] Using a microgrooved surface to promote healing by encouraging migration of cells from adjacent healthy tissue has also been successfully applied to dental and bone implants.[15,16] Although patterned grooved surfaces do increase overall surface roughness, Dibra et al[17] demonstrated that stents with unpatterned microroughened surfaces have no significant influence on coronary restenosis or thrombogenicity

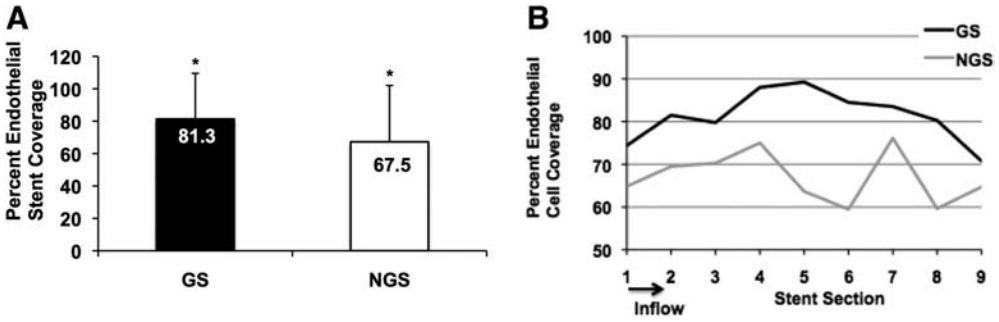

Figure 5. **A**, Relative average endothelial coverage across grooved (GS) and nongrooved (NGS) stents 3 days after stent placement in the right coronary artery or left anterior descending coronary artery. Values are expressed as mean±SD; n=8; **P*<0.001. **B**, Line plot of the percent endothelial coverage at each of the 9 sections along the stents. All levels had greater coverage on GS compared with NGS.

compared with smooth surface stents in a clinical study involving 200 patients.

In the present study, we demonstrate that applying a parallel microgrooved pattern to a stent material surface effectively enhances migration of adjacent arterial wall endothelium on to those areas in vitro. Specifically, our results indicate that the migration rate of HAEC from an intact endothelial surface on to a grooved surface is approximately double that measured for smooth surfaces. Interestingly, the calculated endothelial migration rate of 21 μm/h across the grooved surfaces is comparable to the EC migration rate (25 μm/h) reported for HAEC on stent material under aortic flow conditions.[10] Furthermore, we demonstrate that this increased rate of reestablishment of an intact endothelium on grooved stent surfaces is maintained in vivo and is associated with a decrease in intimal hyperplasia compared with arteries receiving similar stents with no surface patterning in a porcine coronary model of restenosis.

Along with increased endothelialization rates, the migrating endothelial cells on grooved surfaces exhibit key indicators of improved functionality compared with those on smooth surfaces. Insights to the functionality of HAEC cells residing on these surfaces can be ascertained from the increased rates of cell proliferation, NO production, and decreased apoptosis rates observed. The lower HAEC apoptosis rate detected in this study on the grooved surfaces may be mechanistically associated to physical changes in cell shape and size induced by the groove design initiating cell adhesion integrin-mediated signal transduction pathways.[18] Using patterned adhesion molecule substrates to precisely control cell shape and size, Chen et al[19,20] have demonstrated that cells exhibiting greater spreading exhibit decreased rates of apoptosis. Finally, the observation that ECs residing on the grooved surfaces did not exhibit expression of the proinflammatory markers (VCAM-1 or TNF-α) indicates that these cells maintain the anti-inflammatory phenotype characteristic of functional arterial endothelium. Also, our data show that cells that have migrated onto grooved surfaces exhibit increased NO production. The primary cytokine mediating the arterial response to acetylcholine challenging is known to be NO.[21] Several studies have provided evidence that directly applied or endothelial-secreted NO limits vascular smooth

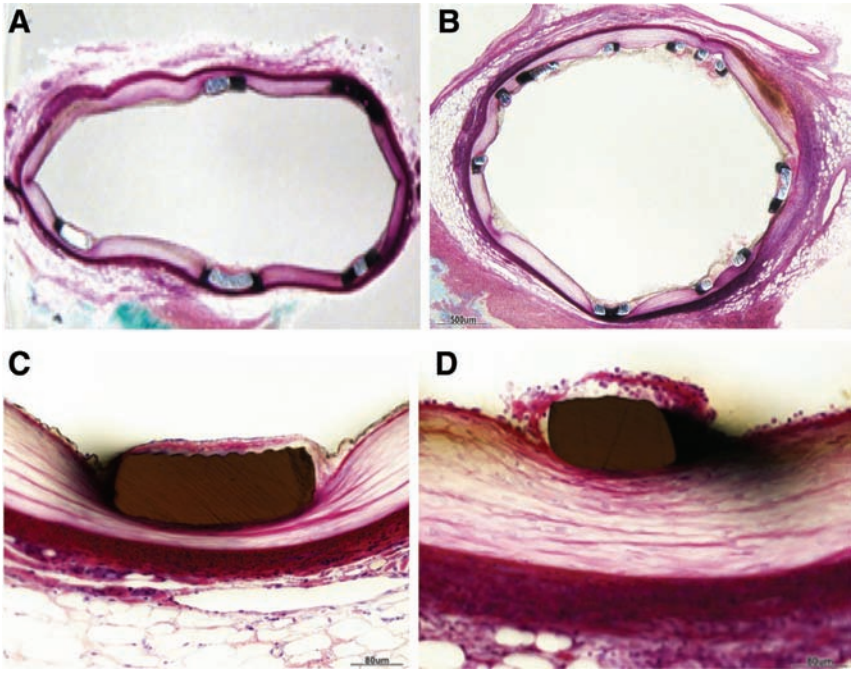

Figure 6. **A** and **B**, Photomicrograph of full cross sections at comparable level of the grooved stent (GS) (**A**) and nongrooved stent (NGS) (**B**) 3 days after placement. Note intact endothelium on GS and lack thereof with mononuclear cells on the NGS stent struts. **C** and **D**, Photomicrograph of histological cross sections of a strut at comparable levels of GS (**C**) and NGS (**D**) 3 days after placement. The intima is completely covered by endothelial cells on top of the GS and incompletely on the NGS strut. Inflammatory cells are present in the immature intimal tissue covering the NGS strut. Endothelium is stained with silver nitrate.

Table 1. Outcome Analysis (28-Day Study) Comparing Histological Results Obtained in Coronary Arteries Stented With GS or NGS

	GS	NGS	Paired *t* Test *P* Value	Wilcoxon Signed-Rank *P* Value
Intimal area, μm²	0.89±0.35	1.12±0.49	0.014	0.021
Intimal thickness, μm	114.4±48.7	148.8±75.3	0.012	0.019
Lumen diameter, mm	2.39±0.13	2.30±0.21	0.034	0.083
Percent diameter stenosis	16.61±6.64	21.37±10.73	0.013	0.029
Stent diameter, mm	2.61±0.09	2.61±0.10	0.691	0.538
Injury score	0.16±0.36	0.05±0.22	0.044	0.045
Inflammation score	0.26±0.50	0.18±0.45	0.373	0.405
Fibrin score	0.13±0.33	0.11±0.31	0.571	0.706

GS indicates grooved stent; NGS, nongrooved stent.
Results are expressed as averages ±SD (n=8).

muscle cell proliferation and migration as well as thrombosis, the key elements involved in intimal hyperplasia leading to eventual restenosis.[22–27] The accelerated reestablishment of an intact and functional endothelial layer promoted by the grooved surfaces appears to increase NO production with important implications for limiting thrombosis at stented sites.

The in vivo (3-day) endothelialization study showed that implantation of GS significantly increased stent surface endothelialization along the entire stent length compared with matched NGS. The high levels of EC coverage observed in both groups underscore the fact that endothelialization in a normal porcine artery is a fast and dynamic process. This rapid rate of reendothelialization in the porcine coronary artery model has been well established and thus assessment at 3 days is required to detect differences with maximum sensitivity. Major differences could be expected in the presence of an atherosclerotic substrate. The longer assay period used our in vitro migration studies performed under static flow conditions are designed to predict relative rates of endothelial migration on different stent substrates. At 28 days, GS displayed a significant decrease in neointimal hyperplasia and percent area of stenosis compared with the paired NGS or MLVS groups. Specifically, the decrease in neointimal area and thickness of the GS in the order of 30% was consistent when compared with both an identical NGS control and the MLV stent. This further supports the hypothesis that rapid surface endothelialization leads to suppression of neointimal formation. Several studies suggest that facilitating EC colonization decreases both thrombus and inflammatory cell attachment, resulting in lower neointimal proliferation.[28,29] Early studies using the rat carotid injury model demonstrated that intimal hyperplasia was increased on removal of the endothelium and was limited by its restoration.[30] Studies using more complex large animal angioplasty models have confirmed the capability of the endothelium to limit restenosis associated with excessive intimal hyperplasia.[5-7]

Our approach to achieving rapid restoration of an intact functional endothelium at revascularization sites has been to provide a defined grooved stent topography to direct and facilitate migration of adjacent arterial endothelium into the stented area. The importance of achieving an increase rate of surface endothelialization is recognized by several other novel approaches toward the same goal. In contrast to deriving endothelial coverage from adjacent endothelium, another technological approach has employed a modified surface to attract blood-derived endothelial progenitor cells (EPC) through surface immobilization of human anti-CD34 antibodies. Similarly, Lim et al[31] used a stent coated with an antibody to vascular endothelial cadherin to capture an EPC subpopulation of more mature or "late" EPCs from circulating blood. Using this stent, a significant reduction in intimal

Table 2. Outcome Analysis (28-Day Study) Comparing Histological Results Obtained in Coronary Arteries Stented With GS or Multi-Link Vision Stent

	GS	MLVS	Paired *t* Test *P* Value	Wilcoxon Signed-Rank *P* Value
Intimal area, μm²	1.58±0.	2.26±1.78	0.012	0291
Intimal thickness, μm	208.4±121	352.2±371.7	0.014	0291
Lumen diameter, mm	2.25±0.23	2.00±0.67	0.026	061
Percent diameter stenosis	27.8±14.3%	37.8±26.0	0.012	0291
Stent diameter, mm	2.67±0.15	2.71±0.12	0.172	611
Injury score	0.05±0.22	0.61±1.11	0.006	008
Inflammation score	0.42±0.059	0.95±1.02	0.013	016
Fibrin score	0.026±0.16	0.13±0.34	0.043	045

GS indicates grooved stent; MLVS, Multi-Link Vision Stent.
Results are expressed as averages ±SD (n=8).

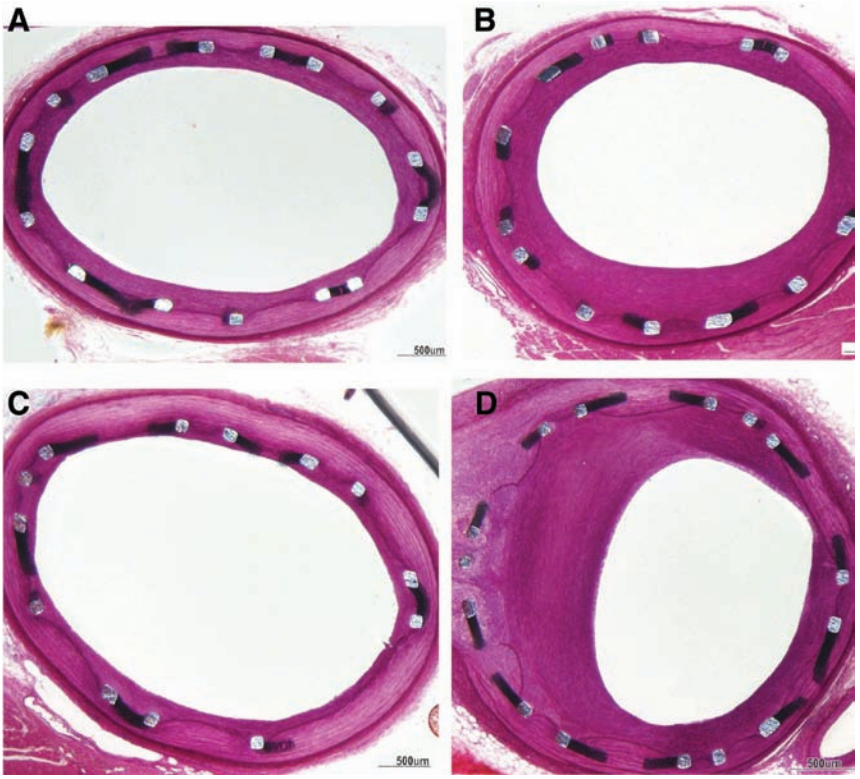

Figure 7. Photomicrographs of histological cross sections at comparable levels of the grooved stent (**A**) and nongrooved stent (**B**) in the left anterior descending coronary artery (LAD) and right coronary artery (RCA), respectively, at 28 days. **C** and **D**, Photomicrographs of histological cross sections at comparable levels of the grooved stent (**C**) and Multi-Link Vision stent (**D**) in the LAD and RCA, respectively, at 28 days.

hyperplasia in rabbit iliac arteries compared with the placement of uncoated stents was observed.[31] Early clinical trials using anti-CD34–coated stents reported favorable stent coverage and comparable safety and restenosis rates compared with bare metal stent controls.[7,32] However, compared with DES, the overall restenosis rates observed is within the range of bare metal stents.[33,34] The lack of any apparent advantage of the early stent endothelialization seen with this technology may be related to the nature of the coating or the cells attracted early to the cell surface. In a recent study, Granada et al[35] demonstrated that by adding an abluminal bioabsorbable sirolimus coating onto the anti-CD34 stent platform, inhibition of restenosis and enhanced endothelialization could be achieved.

Although the animal studies demonstrated overall favorable outcomes using the GS technology, it may be possible that the results will be different when applied to a disease state. However, despite the fact stent healing in porcine coronaries occurs earlier than in any disease state, the differences seen in stent coverage between technologies reinforce the beneficial effect on cell migration promoted by the GS technology. In summary, the present study demonstrates that surface modification using a defined pattern of EC-sized parallel grooves enhances endothelial migration and cell functionality in vitro. Most importantly, this study demonstrates that applying this grooved pattern to a bare metal stent surface both enhances the rate of early endothelialization and significantly limits neointimal hyperplasia when implanted in porcine coronary arteries compared with identical unpatterned bare metal stents. Further research is needed to evaluate the clinical implication of these findings, specifically in the setting of disease and drug elution.

Acknowledgments

We acknowledge the excellent technical contributions of Aaron Watson and Jian Luo and the excellent surgical assistance of Patricia Escobar, DVM.

Sources of Funding

This study was supported by Palmaz Scientific, Inc.

Disclosures

Drs Sprague and Bailey have equity interests in Palmaz Scientific.

References

1. Stone GW, Ellis SG, Colombo A, Grube E, Popma JJ, Uchida T, Bleuit JS, Dawkins KD, Russell ME. Long-term safety and efficacy of paclitaxel-eluting stents final 5-year analysis from the taxus clinical trial program. *J Am Coll Cardiol Cardiovasc Interv*. 2011;4:530–542.
2. Joner M, Finn AV, Farb A, Mont EK, Kolodgie FD, Ladich E, Kutys R, Skorija K, Gold HK, Virmani R. Pathology of drug-eluting stents in humans: delayed healing and late thrombotic risk. *J Am Coll Cardiol*. 2006;48:193–202.
3. Granada JF, Alviar CL, Wallace-Bradley D, Osteen M, Dave B, Tellez A, Win HK, Kleiman NS, Kaluza GL, Lev EI. Patterns of activation and deposition of platelets exposed to the polymeric surface of the paclitaxel eluting stent. *J Thromb Thrombolysis*. 2010;29:60–69.
4. Hofma SH, van der Giessen WJ, van Dalen BM, Lemos PA, McFadden EP, Sianos G, Ligthart JM, van Essen D, de Feyter PJ, Serruys PW. Indication of long-term endothelial dysfunction after sirolimus-eluting stent implantation. *Eur Heart J*. 2006;27:166–170.
5. Garg S, Serruys PW. Coronary stents: looking forward. *J Am Coll Cardiol*. 2010;56:S43–S78.
6. Lemesle G, Maluenda G, Collins SD, Waksman R. Drug-eluting stents: issues of late stent thrombosis. *Cardiol Clin*. 2010;28:97–105.
7. Co M, Tay E, Lee CH, Poh KK, Low A, Lim J, Lim IH, Lim YT, Tan HC. Use of endothelial progenitor cell capture stent (genous bio-engineered r stent) during primary percutaneous coronary intervention in acute myocardial infarction: intermediate- to long-term clinical follow-up. *Am Heart J*. 2008;155:128–132.

8. Palmaz JC, Benson A, Sprague EA. Influence of surface topography on endothelialization of intravascular metallic material. *J Vasc Interv Radiol*. 1999;10:439–444.
9. Bailey SR, Fuss C, Palmaz JC, Sprague EA. Surface micro grooves (MG) improve endothelialization rate in vitro and in vivo. *J Am Coll Cardiol.* 2001;37:70A.
10. Sprague EA, Luo J, Palmaz JC. Human aortic endothelial cell migration onto stent surfaces under static and flow conditions. *J Vasc Intervent Radiol*. 1997;8:83–92.
11. Aravindan N, Mohan S, Herman TS, Natarajan M. Nitric oxide-mediated inhibition of NFkappaB regulates hyperthermia-induced apoptosis. *J Cell Biochem*. 2009;106:999–1009.
12. Hamuro M, Polan J, Natarajan M, Mohan S. High glucose induced nuclear factor kappa B mediated inhibition of endothelial cell migration. *Atherosclerosis*. 2002;162:277–287.
13. Schwartz RS, Edelman ER, Carter A, Chronos N, Rogers C, Robinson KA, Waksman R, Weinberger J, Wilensky RL, Jensen DN, Zuckerman BD, Virmani R. Drug-eluting stents in preclinical studies: recommended evaluation from a consensus group. *Circulation*. 2002;106:1867–1873.
14. Baber U, Mehran R, Sharma SK, Brar S, Yu J, Suh JW, Kim HS, Park SJ, Kastrati A, de Waha A, Krishnan P, Moreno P, Sweeny J, Kim MC, Suleman J, Pyo R, Wiley J, Kovacic J, Kini AS, Dangas GD. Impact of the everolimus-eluting stent on stent thrombosis: a meta-analysis of 13 randomized trials. *J Am Coll Cardiol*. 2011;58:1569–1577.
15. Chehroudi B, McDonnell D, Brunette DM. The effects of micromachined surfaces on formation of bonelike tissue on subcutaneous implants as assessed by radiography and computer image processing. *J Biomed Mater Res*. 1997;34:279–290.
16. Frenkel SR, Simon J, Alexander H, Dennis M, Ricci JL. Osseointegration on metallic implant surfaces: effects of microgeometry and growth factor treatment. *J Biomed Mater Res*. 2002;63:706–713.
17. Dibra A, Kastrati A, Mehilli J, Pache J, von Oepen R, Dirschinger J, Schomig A. Influence of stent surface topography on the outcomes of patients undergoing coronary stenting: a randomized double-blind controlled trial. *Catheter Cardiovasc Interv*. 2005;65:374–380.
18. Bhadriraju K, Yang M, Alom Ruiz S, Pirone D, Tan J, Chen CS. Activation of rock by rhoa is regulated by cell adhesion, shape, and cytoskeletal tension. *Exp Cell Res*. 2007;313:3616–3623.
19. Chen CS, Mrksich M, Huang S, Whitesides GM, Ingber DE. Geometric control of cell life and death. *Science*. 1997;276:1425–1428.
20. Chen CS, Mrksich M, Huang S, Whitesides GM, Ingber DE. Micropatterned surfaces for control of cell shape, position, and function. *Biotechnol Prog*. 1998;14:356–363.
21. Amezcua JL, Dusting GJ, Palmer RM, Moncada S. Acetylcholine induces vasodilatation in the rabbit isolated heart through the release of nitric oxide, the endogenous nitrovasodilator. *Br J Pharmacol*. 1988;95:830–834.
22. Colotti C, Vittorini S, Ottaviano V, Maltinti M, Angeli V, Del Ry S, Giannessi D. Nitric oxide treatment reduces neo-intimal formation and modulates osteopontin expression in an ex-vivo human model of intimal hyperplasia. *Cytokine*. 2009;46:228–235.
23. Fischer JW, Hawkins S, Clowes AW. Pharmacologic inhibition of nitric oxide synthases and cyclooxygenases enhances intimal hyperplasia in balloon-injured rat carotid arteries. *J Vasc Surg*. 2004;40:115–122.
24. Garanich JS, Pahakis M, Tarbell JM. Shear stress inhibits smooth muscle cell migration via nitric oxide-mediated downregulation of matrix metalloproteinase-2 activity. *Am J Physiol Heart Circ Physiol*. 2005;288:H2244–H2252.
25. Groves PH, Banning AP, Penny WJ, Newby AC, Cheadle HA, Lewis MJ. The effects of exogenous nitric oxide on smooth muscle cell proliferation following porcine carotid angioplasty. *Cardiovasc Res*. 1995;30:87–96.
26. Kaul S, Cercek B, Rengstrom J, Xu XP, Molloy MD, Dimayuga P, Parikh AK, Fishbein MC, Nilsson J, Rajavashisth TB, Shah PK. Polymeric-based perivascular delivery of a nitric oxide donor inhibits intimal thickening after balloon denudation arterial injury: role of nuclear factor-kappaB. *J Am Coll Cardiol*. 2000;35:493–501.
27. Kibbe MR, Tzeng E, Gleixner SL, Watkins SC, Kovesdi I, Lizonova A, Makaroun MS, Billiar TR, Rhee RY. Adenovirus-mediated gene transfer of human inducible nitric oxide synthase in porcine vein grafts inhibits intimal hyperplasia. *J Vasc Surg*. 2001;34:156–165.
28. Allaire E, Clowes AW. Endothelial cell injury in cardiovascular surgery: the intimal hyperplastic response. *Ann Thorac Surg*. 1997;63:582–591.
29. Kolandaivelu K, Swaminathan R, Gibson WJ, Kolachalama VB, Nguyen-Ehrenreich KL, Giddings VL, Coleman L, Wong GK, Edelman ER. Stent thrombogenicity early in high-risk interventional settings is driven by stent design and deployment and protected by polymer-drug coatings. *Circulation*. 2011;123:1400–1409.
30. Clowes AW, Clowes MM, Fingerle J, Reidy MA. Regulation of smooth muscle cell growth in injured artery. *J Cardiovasc Pharmacol*. 1989;14:S12–S15.
31. Lim WH, Seo WW, Choe W, Kang CK, Park J, Cho HJ, Kyeong S, Hur J, Yang HM, Lee YS, Kim HS. Stent coated with antibody against vascular endothelial-cadherin captures endothelial progenitor cells, accelerates re-endothelialization, and reduces neointimal formation. *Arterioscler Thromb Vasc Biol*. 2011;31:2798–2805.
32. Aoki J, Serruys PW, van Beusekom H, Ong AT, McFadden EP, Sianos G, van der Giessen WJ, Regar E, de Feyter PJ, Davis HR, Rowland S, Kutryk MJ. Endothelial progenitor cell capture by stents coated with antibody against CD34: the HEALING-FIM (Healthy Endothelial Accelerated Lining Inhibits Neointimal Growth-First In Man) Registry. *J Am Coll Cardiol*. 2005;45:1574–1579.
33. Klomp M, Beijk MA, Varma C, Koolen JJ, Teiger E, Richardt G, Bea F, van Geloven N, Verouden NJ, Chan YK, Woudstra P, Damman P, Tijssen JG, de Winter RJ. One-year outcome of TRIAS HR (Tri-Stent Adjudication Study-High Risk of Restenosis): a multicenter, randomized trial comparing genous endothelial progenitor cell capturing stents with drug-eluting stents. *J Am Coll Cardiol Cardiovasc Interv*. 2011;4:896–904.
34. van Beusekom HM, Ertas G, Sorop O, Serruys PW, van der Giessen WJ. The genous endothelial progenitor cell capture stent accelerates stent re-endothelialization but does not affect intimal hyperplasia in porcine coronary arteries. *Catheter Cardiovasc Interv*. 2011;79:231–242.
35. Granada JF, Inami S, Aboodi MS, Tellez A, Milewski K, Wallace-Bradley D, Parker S, Rowland S, Nakazawa G, Vorpahl M, Kolodgie FD, Kaluza GL, Leon MB, Virmani R. Development of a novel prohealing stent designed to deliver sirolimus from a biodegradable abluminal matrix. *Circ Cardiovasc Interv*. 2010;3:257–266.